Contribution to the Chemistry of Boron, 238[◇]

Synthesis and Assembly Mechanism for Spirocyclic Cage Compounds Containing B, P and Si Atoms

Tuqiang Chen[a], Eileen N. Duesler[a], Robert T. Paine*[a], and Heinrich Nöth*[b]

Department of Chemistry, University of New Mexico[a],
Albuquerque, New Mexico 87131-1096, USA

Institut für Anorganische Chemie, Universität München[b],
D-80333 München, Germany

Received January 2, 1997

Keywords: Boron / Phosphorus / Spiro compounds / Cage compounds

Reactions of 1-lithio · DME-2,4-bis(dialkylamino)-1,3,2,4-diphosphadiboretanes (**1a**, **1b**) with $SiCl_4$ followed by dehydrohalogenation with *t*BuLi produce spirocyclic compounds $[(R_2NB)_2P_2]_2Si$ (**2a**, **2b**). The compounds have been characterized by spectroscopic methods and X-ray crystallography. The assembly process has also been followed and one intermediate species $[(iPr_2NB)_2P_2][(iPr_2NB)P(H)(iPr_2NB)P]SiCl$ (**3**) has been isolated and fully characterized.

Introduction

The development of efficient syntheses for new phosphinoborane ring compounds is allowing for extensive studies of their reaction chemistry[2]. It has been found, for example, that 1,3,2,4-diphosphadiboretanes are useful starting points in the synthesis of a family of five- and six-vertex cage species of the general types $(R_2NB)_2P_2(E)$, E = R_2NB[3], R_2Si[4], R_2Ge[5] and R_2Sn[6], and $(R_2NB)_2P_2(E_2)$, $E_2 = Me_2SiSiMe_2$[4]. It has also been found that larger cage compounds can be made in a stepwise assembly approach and a 14-vertex species, $\{[iPr_2NB)_2P_2Si]_2[(R_2NB)_2P_2]\}$, has been structurally characterized[7]. This report describes the extension of this chemistry to the formation of new spirocyclic containing nine-vertex atoms.

Reactions

The 2:1 combinations of the Li salts **1a** and **1b**, with $SiCl_4$ followed by treatment with two equivalents of *t*BuLi produce colorless (**2a**) and pale yellow (**2b**) crystalline solids as summarized in equation 1.

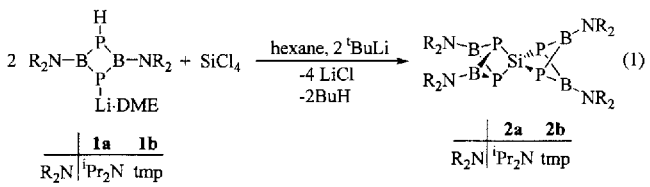

(1)

The compounds are formed in high yield as indicated by ^{31}P-NMR analysis of the reaction mixtures; however, they are isolated in only moderate yield due to their high solubility in common organic solvents. They are moisture sensitive, but stable toward dry air. The compounds act as ligands toward metal carbonyl fragments; however, more than one complex is obtained, and these could not be adequately separated and characterized.

The process by which **2a** and **2b** form is of interest in the context of our attempts to develop systematic syntheses for more complex cage molecules. As a result, the reactions of **1a** and **1b** with $SiCl_4$ were examined with several reagent stoichiometries and reaction conditions. It was expected that the 2:1 reaction of **1a** or **1b** with $SiCl_4$ would proceed by a double chloride displacement process producing bis[2,4-bis(dialkylamino)-1,3,2,4-diphosphadiboretanyl]dichloro-silanes **4** as shown in Scheme 1.

This compound would be anticipated to undergo subsequent double intramolecular dehydrohalogenation with cage closures to give **2a** or **2b**. However, in practice, the 2:1 reactions give several products as shown by ^{31}P-NMR analysis. For example, the combination of **1a** (R_2N = iPr_2N) with $SiCl_4$ in hexane forms the known parent diphosphadiboretane[8], $(iPr_2NBPH)_2$ (**1a** + **H**) (^{31}P: δ = −164), **3a**, (^{31}P: δ = 14.9, −109.9, −147.5, $^1J_{PH}$ = 197 Hz), **6a** (^{31}P: δ = 18.3) and **4a** (^{31}P: δ = −127.3, −149.0, $^1J_{PH}$ = 198 Hz, $^2J_{PP'}$ = 51 Hz) with relative amounts (**1a** + **H**) > **3a** ≅ **6a** > **4a**. Treatment of this reaction mixture with an additional equivalent of **1a** (total three equivalents) gives a significantly increased yield of (**1a** + **H**) and **3a** as well as a small amount of the final cage species **2a**. Numerous attempts to separate and purify the individual components by fractional recrystallization were unsuccessful. Mass spectra recorded from various samples show intense ion envelopes that correspond to the parent ions for **4**, (**1a** + **H**) and **6a**, although the envelopes for the latter two could conceivably originate from fragment ions of **4a**. A high resolution M.S.

[◇] Part 237: See ref.[1].

  0009–2940/97/0707–0933 $ 15.00+.25/0

Scheme 1

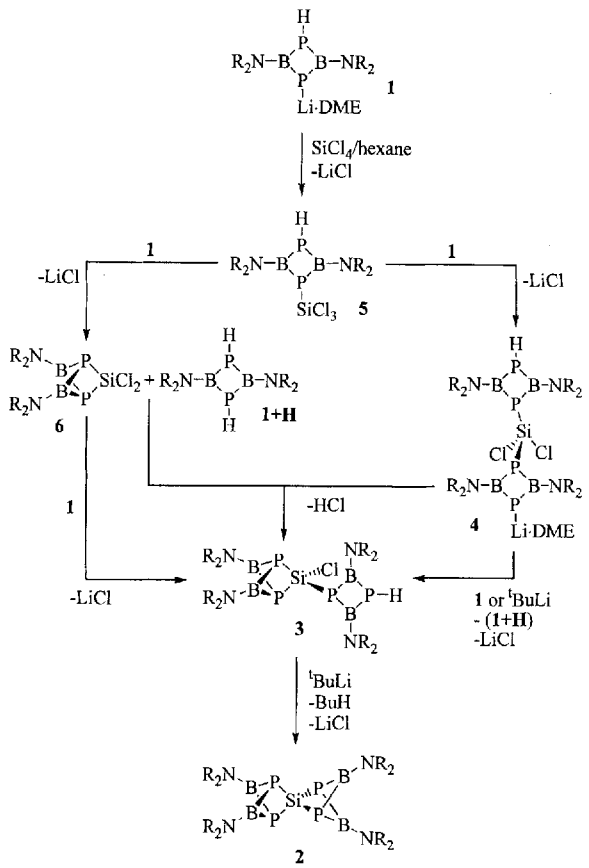

for a sample containing **4a** shows a parent ion consistent with the molecular formula $^{12}C_{24}H_{58}{}^{11}B_4{}^{14}N_4{}^{28}Si^{31}P_4{}^{35}Cl_2$: calcd. 668.31302; found 668.31203, dev. −1.5 ppm. Attempts to derivatize **4a** and **6a** by reaction of the product mixtures with organometallic reagents and amines did not provide pure component derivatives.

The direct reaction of three equivalents of **1a** with $SiCl_4$ in hexane produces a simpler mixture containing only the known (**1a** + **H**) and **3a**. The differences in solubility for these compounds allows for separation and purification of **3a** from cold pentane although the recrystallizations result in relatively low final yields. Compound **3a** is obtained as moisture-sensitive pale yellow crystals. In addition, equimolar reactions of pure samples of **3a** with *t*BuLi (Method B) or **1a** produce the cage compound **2a**.

Taken together, these observations are consistent with the processes outlined in Scheme 1. The initial equivalent of the phosphido salt **1a** appears to react with $SiCl_4$ to produce **5a**, which at this time has eluded isolation. This compound apparently takes part in two reaction pathways in the presence of an additional equivalent of **1a**. It either undergoes Cl substitution on **5a** to give **4a**, or promotes intramolecular dehydrogenation to produce **6a** and (**1a** + **H**). Although **4a**, **5a** and **6a** are not fully characterized here, their ^{31}P-NMR spectra are consistent with the proposed structures. Compound **6a** would react by Cl displacement while **4a** would undergo dehydrohalogenation with single cage closure. Indeed, treatment of the mixture containing **4a**, **6a** and (**1a** + **H**) with a third equivalent of **1a** gives rise to Cl substitution on **6a** and intramolecular dehydrohalogenation on **4a**, producing the same product **3a** but by different pathways. Finally, treatments of pure samples of **3a** or mixtures containing **3a** with *t*BuLi give the "double cage" compound **2a**. These processes are also consistent with the sequential reaction of $SiCl_4$ with two equivalents of **1a** followed by two equivalents of *t*BuLi in which one equivalent of *t*BuLi simply deprotonates (**1a** + **H**) formed in the 2:1 reaction of **1a** and $SiCl_4$. The isolation and characterization of the key intermediate **3a** along with the NMR data assigned to **4a** and **6a** provide solid evidence for the combination of processes represented in Scheme 1.

Spectroscopic Characterization Data

NMR Spectra: The ^1H, ^{13}C, ^{11}B and ^{31}P chemical shifts and coupling constants are summarized in the expermental part and several specifics are worth discussion. The "double cage" compounds **2a** and **2b** display a single low field ^{31}P-NMR resonance centered at $\delta = -6.5$ and 38.9, respectively. These shifts are similar to values reported for $P_2(iPr_2NB)_2SiPh_2$ ($\delta = -18.4$), $P_2(tmpB)_2SiMe_2$ ($\delta = 3.13$) and $P_2(tmpB)_2SiPh_2$ ($\delta = 32.2$)[4]. In all $P_2(R_2NB)_2E$ species, the ^{31}P chemical shift for derivatives containing iPr_2NB fragments appear at higher fields relative to those with tmpB fragments[1]. The ^{11}B-NMR spectra display a single resonance at $\delta = 45.7$ and 48.6, respectively, and these compare well with ^{11}B-NMR data for the five-vertex cage molecules[4]. The ^1H-NMR spectrum for **2a** at 22°C shows two doublets centered at $\delta = 1.30$ and 1.31, $^3J_{PH} = 6.7$ Hz, that are assigned to inequivalent *i*Pr groups on each amino fragment, with the inequivalence caused by hindered rotation about the C−N bonds. The two doublets collapse into a single doublet at 37°C consistent with $\Delta G^{+} \approx 17$ kcal/mol. One *i*Pr C−H multiplet resonance is displayed in the spectrum. The $^{13}C\{^1H\}$-NMR spectrum of **2a** also displays inequivalent Me group environments and equivalent C−H groups at 22°C. The ^1H and ^{13}C spectra involving the tmp rings of **2b** are typically complicated and full assignment of the peaks was not conducted.

The ^{31}P-NMR spectrum for **3a** (R_2N = *i*PrN) contains three resonances centered at $\delta = 14.9$, −109.9 and −147.5 with a 2:1:1 area ratio. Based upon the peak intensities and shift positions, the lowest field resonance is assigned to the apical P atoms P(3) and P(4) that are part of the five-atom cage fragment. The highest field resonance is split into a doublet of doublets $^1J_{PH} = 197$ Hz and $^2J_{PP} = 52$ Hz, and it is assinged to P(2). The remaining resonance, a doublet at $\delta = -109.9$, $^2J_{PP} = 52$ Hz, is assigned to P(1). These shifts are in the general ranges expected for B_2PH and B_2PSi fragments[1,4]. It might be anticipated that three inequivalent boron environments would exist in **3a**, but in fact only two resonances are resolved at $\delta = 46.9$ and 44.3. The ^1H- and ^{13}C-NMR data clearly show inequivalent Me and CH environments, although correlation spectra have not been recorded to fully assign the resonances to specific

*i*Pr groups. The doublet of doublets resonance for the P–H group is resolved at $\delta = 4.6$, $^1J_{PH} = 198$ Hz, $^3J_{PH} = 14$ Hz.

Infrared Spectra: The infrared spectra of **2a**, **2b** and **3a** have been recorded and the principle bands are listed in the experimental part. The spectra of **2a** and **2b** are very similar to those of the five- and six-vertex cages $P_2(R_2NB)_2SiR_2'$ and $P_2(R_2NB)_2Si_2R'_4$[4]. The spectrum of **3a** is similar to other silylated diphosphadiboretanes[4] and the ν_{PH} band appears at 2288 cm^{-1}.

Mass Spectra: The mass spectra of **2a**, **2b** and **3a** display a parent ion envelope and in each case the parent envelope is the most intense. In the spectra for **2a** and **2b** there are no other ions of significant intensity displayed. A high-resolution EI-MS was obtained for **2a** and it gives a molecular weight for $^{12}C_{24}H_{56}{}^{10}B^{11}B_3{}^{14}N_4{}^{28}Si^{31}P_4$ 595.36300 (dev. −0.5 ppm from calculated MW).

Molecular Structures

The spectroscopic data are consistent with but do not provide unambiguous proof for the proposed structures of **2a**, **2b** and **3a**. Since the compounds represent new cage types and a key intermediate in a cage assembly process, the molecular structures have been examined by single crystal X-ray methods. Views of compounds **2a** and **2b** (molecule 1) are shown in Figures 1 and 2.

Figure 1. Molecular structure and atom labeling scheme for **2a**[a]

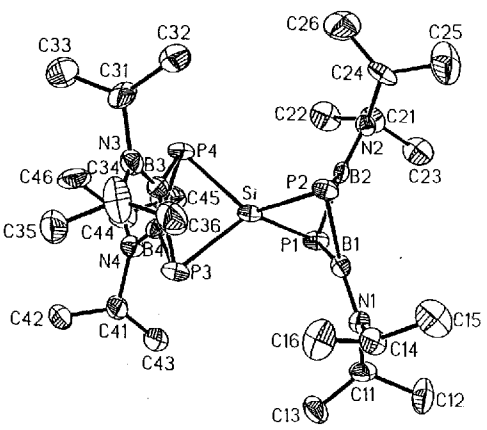

[a] H atoms omitted for clarity; thermal ellipsoids represented at 30% probability level; selected bond lengths [Å]: Si–P(1) 2.233(7), Si–P(2) 2.254(7), Si–P(3) 2.248(6), Si–P(4) 2.256(7), P(1)–B(1) 1.96(1), P(1)–B(2) 1.97(2), P(2)–B(1), 2.02(2), P(2)–B(2) 1.96(2), P(3)–B(3) 1.99(2), P(3)–B(4) 1.92(2), P(4)–B(3) 1.94(2), P(4)–B(4) 1.97(2), B(1)–N(1) 1.37(2), B(2)–N(2) 1.39(2), B(3)–N(3) 1.40(3), B(4)–N(4) 1.40(2).

Both compounds have a nine-vertex spirocyclic cage structure in which two $P_2(R_2NB)_2Si$ five-vertex polyhedra are joined at and share a common vertex Si atom. The crystal quality in both compounds is not optimal. In the case of **2a**, the *i*PrN group containing N(3), C(31) and C(34) is disordered, and in **2b** there are two crystallographically independent molecules in the unit cell, and a solvent molecule (Et_2O) in the lattice that is disordered. These factors influence the level of accuracy of the refined parameters, but the crucial information regarding the molecular structures is not compromised. For example, the bond lengths and angles in the individual five-vertex trigonal bypyramids of **2a** and **2b** are similar to $P_2(iPr_2NB)_2SiPh_2$ (**7**)[4] and $P_2(tmpB)_2SiPh_2$ (**8**)[4]. The average *endo* P–Si–P bond angle, **2a** (85.0°) and **2b** (83.9°), are acute compared to the average *exo* P–Si–P bond angles, **2a** (123.0°) and **2b** (123.7°). The apical P atoms have very acute internal angles (average) **2a** (70.7°) and **2b** (72.3°) and these features have also been seen in **7** and **8**. The B and N atoms display trigonal planar geometries and the average B–N distances **2a** (1.388 Å) and **2b** (1.377 Å) are comparable with the values in **7** (1.375 Å) and **8** (1.384 Å). The atom geometries and bond distances are consistent with B–N π overlap. The average B–P distances, **2a** (1.966 Å) and **2b** (1.981 Å), are similar to those in **7** (1.973 Å) and **8** (1.992 Å) and they are in the single bond range[2]. The average P–Si bond lengths, **2a** (2.248 Å) and **2b** (2.243 Å), are identical with the values in **7** (2.244 Å) and **8** (2.243 Å) as well as with the average distance in the cage species $P_4(SiMe_2)_6$[9], (2.244 Å). Interestingly, the P–Si distances in **2a** and **2b** are longer than the average distance in the spirocycle $(tBuP)_2Si(tBuP)_2$[10] (2.201 Å), which contains a strained three-membered *cyclo*-[–P–Si–P–] ring (average P–Si–P angle, 61.6°).

Figure 2. Molecular structure and atom labeling scheme for **2b**[a]

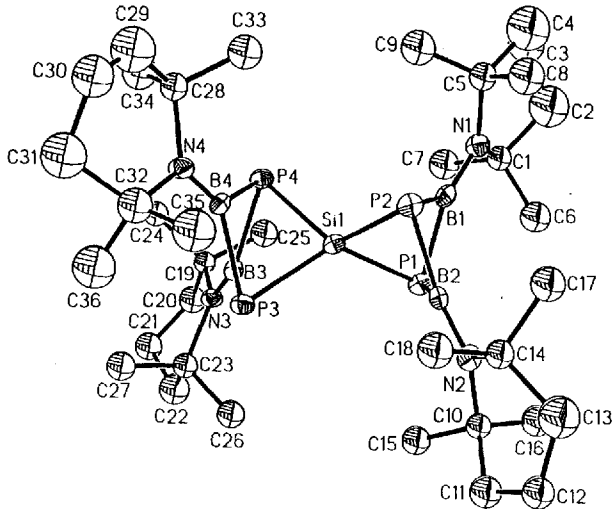

[a] Molecule 1, H atoms omitted for clarity; thermal ellipsoids represented at 30% probability level; selected bond lengths [Å]: Si–P(1) 2.230(6), Si–P(2) 2.231(7), Si–P(3) 2.250(7), Si–P(4) 2.263(6), P(1)–B(1) 1.99(2), P(1)–B(2) 1.96(2), P(2)–B(1) 2.00(2), P(2)–B(2) 1.96(2), P(3)–B(3) 1.97(2), P(3)–B(4) 2.00(2), P(4)–B(3) 1.99(2), P(4)–B(4) 1.97(2), B(1)–N(1) 1.37(3), B(2)–N(2) 1.41(2), B(3)–N(3) 1.38(2), B(4)–N(4) 1.35(2).

The molecular structure of **3a** is depicted in Figure 3.

The structure consists of a five-vertex trigonal bypyramidal $P_2(iP_2NB)_2Si$ cage fragment and a four-atom 1,3,2,4-diphosphadiboretane B_2P_2 ring fragment joined through a P–Si bond. The Si atom also possesses a terminal Cl atom. This is the structure proposed for the intermediate in Scheme 1. The structure of the P_2B_2Si cage in **3a** is closely related to the structures discussed above. In particular, the internal P(3)–Si–P(4) angle, [84.6(1)°], and the average in-

Figure 3. Molecular structure and atom labeling scheme for **3a**[a]

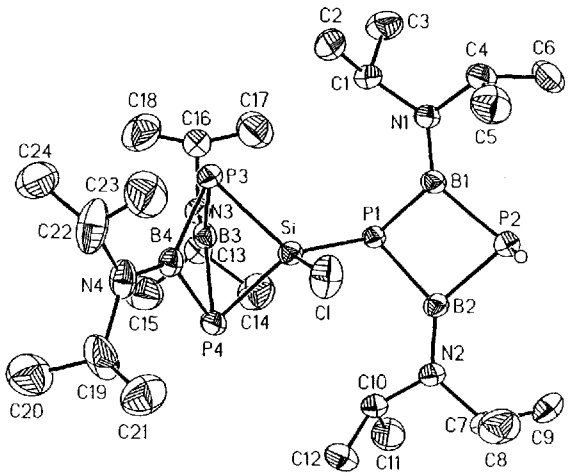

[a] H atoms omitted for clarity except on P(2); thermal ellipsoids represented at 30% probability level; selected bond lengths [Å]: Si–Cl 2.088(1), Si–P(1) 2.224(1), Si–P(3) 2.239(1), Si–P(4) 2.245(1), P(1)–B(1) 1.965(3), P(1)–B(2) 1.969(4), P(2)–B(1) 1.932(4), P(2)–B(2) 1.928(4), P(3)–B(3) 1.962(4), P(3)–B(4) 1.958(5), P(4)–B(3) 1.966(5), P(4)–B(4) 1.966(4), B(1)–N(1) 1.374(5), B(2)–N(2) 1.370(5), B(3)–N(3) 1.415(4), B(4)–N(4) 1.378(5).

ternal angles at the apical P atoms, (71.0°), the average B–P distance, (1.966 Å), and the average P–Si distance, (2.232 Å), are all comparable with the values in **2a** and **7**. The average B–N distance, 1.395 Å, appears to be slightly longer than in **2a** and **7**, but the N(3) atom involving the longer distance, B(3)–N(3) 1.415(5) Å, is bonded to the disordered *i*Pr substituent. This reduces the accuracy of average value and should not be interpreted to result from a steric or electronic influence.

The unique structural feature in **3a** is the geometry of the P_2B_2 ring. Typically, 1,3,2,4-diphosphadiboretanes such as $(iPr_2NBPH)_2$, $(tmpBPH)_2$ and $(iPr_2NBPSiMe_3)_2$ have a planar ring geometry with the P–H or P–Si substituents *trans* to each other. In the case of **3a**, however, the P_2B_2 ring is folded [B(1)–P(1)–B(2)–P(2) torsion angle = 18.4°] and the P atom substituent groups are *cis* to each other. This is shown more clearly in Figure 4.

Figure 4. Perspective of molecule **3a** showing stereochemical relationship between the P_2B_2 ring and the B_2B_2Si cage

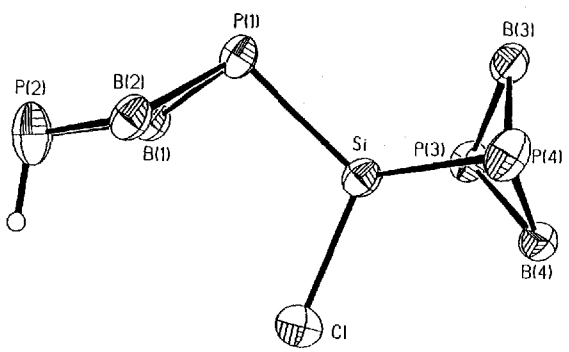

Interestingly, in the solid state this places the P–H group and Si–Cl group on the same side of the P_2B_2 ring, suggesting that the molecule is nicely positioned for HCl elimination. The sum of angles about P(1), (282.3°), is significantly smaller than the sum of angles about P(2), (289.6°), indicating a larger ring strain around P(1). The more strained P(1) atom also exhibits longer B–P bond lengths: $P(1)-B_{avg}$ (1.967 Å), $P(2)-B_{avg}$ (1.930 Å).

The interesting chemistry and structural features presented here provide additional details on factors that influence main group element cage construction processes, and the evolving principles will be helpful in the further design of new families of cage species.

We thank the *National Science Foundation* (CHE-9508668) (RTP) and the *Fonds der Chemischen Industrie* (HN) for financial support of our programs.

Experimental Section

General: All syntheses and product manipulations were performed under dry nitrogen by using Schlenk-type techniques and/or drybox; solvents were dried by standard procedures and stored under N_2. – IR: Mattson 2020-FTIR. – MS: Finnegan GC/MS or Kratos MS-50 with FAB source. – NMR: Bruker WP-250 and JEOL 400 with $^{11}BF_3 \cdot OEt_2$ (external), 85% H_3PO_4 (external) and TMS as references; positive δ values refer to shifts upfield of the reference. – Elemental analyses were performed at the UNM microanalytical facility.

Compounds **2a** *and* **2b**. – *Method A:* $SiCl_4$ (0.23 g, 1.4 mmol) was dissolved in 50 ml of hexane, cooled to −78°C and a solid sample of **1** (1.04 g, 2.7 mmol)[4] was added slowly with stirring. The mixture was stirred at −78°C (2 h) and at 23°C (15 h) and then filtered. The filtrate was cooled to −78°C and *t*BuLi/pentane solution (1.8 ml, 1.7 M, 2.7 mmol) was added dropwise. The mixture was stirred at −78°C (2 h) and 23°C (15 h) and the resulting suspension was filtered and the filtrate vacuum evaporated. The residue was recrystallized from hexane (10 ml) at −10°C as colorless crystals. Yield: 0.39 g of **2a** (48%), m.p. >250°C. Compound **2b** was pepared in an identical fashion from $SiCl_4$ and **1b**, and isolated as pale yellow crystals. Yield: 0.45 g of **2b** (41%), m.p. >250°C. – NMR (C_6D_6): **2a**: ^1H NMR: δ = 1.30 (d, 3H, $^3J_{HH}$ = 6.7 Hz, $CHCH_3$), 1.31 (d, 3H, $^3J_{HH}$ = 6.7 Hz, $CHCH_3$), 3.92 (sept, ^1H, $^3J_{HH}$ = 6.7 Hz, $CHCH_3$); $^{13}C\{^1H\}$ NMR: δ = 23.3 (s, CH_3), 24.2 (s, CH_3), 52.1 (s, CH); $^{11}B\{^1H\}$ NMR: δ = 45.7; $^{31}P\{^1H\}$ NMR: δ = −6.5. – NMR (C_6D_6): **2b**: ^1H NMR: δ = 1.40–1.57 (CH_2), 1.76 (CH_3), 1.78 (CH_3); $^{13}C\{^1H\}$ NMR: δ = 15.7, 34.0 (t, $^4J_{CP}$ = 7.7 Hz), 39.7, 57.8; $^{11}B\{^1H\}$ NMR: δ = 48.6; $^{31}P\{^1H\}$ NMR: δ = 38.9. – IR (cm^{-1}, KBr): **2a**: $\tilde{\nu}$ = 2969 s, 2926 s, 2868 m, 1468 s, 1443 s, 1364 m, 1305 s, 1184 m, 1142 s, 1003 w, 762 w, 558 m, 494 w, 434 w; **2b**: $\tilde{\nu}$ = 2957 s, 2936 s, 2866 m, 1464 m, 1365 s, 1325 s, 1291 s, 1249 m, 1165 s, 1127 m, 1039 w, 990 m, 685 w, 577 w, 509 w. – MS: **2a**: HREI-MS (70 eV): for $^{12}C_{24}H_{56}{}^{10}B^{11}B_3{}^{14}N_4{}^{31}P_4{}^{28}Si$: calcd. 595.36398. found: 595.36300, dev. −0.5 ppm; **2b**: EI-MS (30 eV); *m/z* (%): 754–759 (100) [M^+]. – **2a** $C_{24}H_{56}B_4N_4P_4Si$ (595.96): calcd. C 48.36, H 9.47, N 9.40; found C 48.56, H 9.90, N 9.37.

Method B: To a cooled (−78°C) solution of **3a** (0.40 g, 0.63 mmol) in hexane (30 ml) was added dropwise a *t*BuLi/pentane solution (0.40 ml, 1.7 M, 0.68 mmol). The resulting pale yellow cloudy solution was stirred at −78°C (2 h) and 23°C (15 h) and filtered. The filtrate was evaporated to dryness and the residue extracted with hexane. Recrystallization from hexane (ca. 10 ml) at −10°C gave colorless crystals of **2a**. Yield: 0.20 g of **2a** (59%).

5-Chloro-2,4-bis(diisopropylamino)-5-[2',4'-bis(diisopropylamino)-1',3',2',4'diphosphadiboretanyl]-1,3-diphospha-5-sila-2,4-

Table 1. Crystallographic data for **2a**, **2b** and **3a**

	2a	**2b**	**3a**
Chemical formula	$C_{24}H_{56}B_4N_4P_4Si$	$C_{73}H_{144}B_8N_8O_{0.25}P_8Si_2$	$C_{24}H_{57}B_4N_4P_4SiCl$
Formula weight	595.9	1528.4	632.4
Crystal size [mm]	0.06 × 0.39 × 0.41	0.18 × 0.30 × 0.53	0.23 × 0.34 × 0.69
Crystal system	triclinic	monoclinic	triclinic
Space group	$P\bar{1}$	$P2_1/n$	$P\bar{1}$
a [Å]	10.590(4)	12.062(2)	11.751(1)
b [Å]	10.768(4)	32.940(7)	12.022(1)
c [Å]	19.525(5)	24.429(5)	14.815(1)
α [°]	90.98(4)	90.0	84.22(1)
β [°]	105.64(2)	103.85(3)	73.54(1)
γ [°]	116.92(4)	90.0	70.76(1)
V [Å^3]	1886.5(17)	9411(3)	1894.9(3)
Z	2	4	2
$\rho_{calcd.}$ [g cm^{-3}]	1.048	1.079	1.108
μ [mm^{-1}]	0.245	0.209	0.321
$F(000)$	640	3312	680
Index range	$0 \le h \le 10$, $-11 \le k \le 10$, $-21 \le l \le 20$	$0 \le h \le 11$, $0 \le k \le 31$, $-23 \le l \le 22$	$-1 \le h \le 13$, $-13 \le k \le 14$, $-17 \le l \le 17$
2θ [°]	2-45	2-40	2-50
T [K]	293	293	293
Refl. collected	5109	9523	7741
Refl. unique	4791	8742	6670
Refl. observed	2439 (2σ)	4386 (2σ)	4904 (2σ)
No. variables	334	524	314
Weight. scheme[a] (g)	0.0023	0.0100	0.0010
GOOF	1.39	1.01	1.15
R	0.123	0.107	0.0521
R_w	0.113	0.111	0.0542
Larg. res. peak [eÅ^{-1}]	0.44	1.00	0.47

[a] $w^{-1} = \sigma^2(F) + gF^2$.

diborabicyclo[1.1.1]pentane (**3a**): A solution of $SiCl_4$ (0.27 g, 1.6 mmol) in hexane (30 ml) was cooled to −78°C and a solid sample of **1a** (1.88 g, 4.9 mmol) was added slowly with stirring over 2 h. After the addition was complete, the mixture was stirred at 23°C (24 h), filtered and the filtrate vacuum evaporated leaving a pale yellow residue, which was recrystallized twice from pentane (5 ml) at −10°C leaving pale yellow crystals. Yield: 0.45 g of **3a** (43%), m.p. 190−192°C. − NMR (C_6D_6): ^{1}H NMR: δ = 1.20−1.23 (m, 48H, CHCH_3), 3.25 (m, 2H, CHCH$_3$), 3.83 (m, 4H, CHCH$_3$), 4.46 (m, 2H, CHCH$_3$), 4.61 (d of d, $^1J_{PH}$ = 1.98 Hz, $^3J_{PH}$ = 14 Hz); ^{13}C{^{1}H} NMR: δ = 22.5, 23.6, 24.8 (CH$_3$), 47.6, 52.6, 55.5 (CH); ^{11}B{^{1}H} NMR: δ = 46.9, 44.3; ^{31}P{^{1}H} NMR: δ = 14.9, −109.9, $J_{PP'}$ = 52 Hz), −147.5, (J_{PH} = 197, $J_{PP'}$ = 52 Hz). − IR (cm^{-1}, KBr): $\tilde{\nu}$ = 2967 s, 2929 s, 2868 m, 2288 w, 1468 s, 1445 s, 1364 s, 1310 s, 1182 m, 1144 s, 1003 m, 858 w, 795 w, 575 w, 542 m, 482 w, 444 w. − MS: EI-MS (30 eV); *m/z* (%): 635−629 (100) [M$^+$]. − $C_{24}H_{57}N_4B_4P_4SiCl$ (632.40): calcd. C 45.58, H 9.09, N 8.86; found C 45.18, H 9.59, N 8.39.

X-ray Structure Determinations: Single crystals of **2a**, **2b** and **3a** were mounted in glass capillaries under dry N_2. X-ray data were collected with Mo-K_α radiation on a Siemens R3m/V diffractometer. Computer programs were from Siemens SHELXTL PLUS (VMS version)[11]. The structures were solved by direct methods and non-hydrogen atom positions refined anisotropically. H-atom positions were calculated in idealized positions by using the riding model. Semi-empirical absorption corrections based upon psi-scans were employed. A summary of crystal data is given in Table 1.

Reduced crystal quality hindered the refinement of each compound. **2a** showed no signs of decay, but positional disorder of C(31) and C(34) on N(3) appeared. The H-atom on each of these atoms was not included in the final refinement. **2b** showed no signs of decay, but it diffracted weakly. The crystal contains two independent molecules in the asymmetric unit and a molecule of Et_2O per unit cell which was disordered. Only the Si, P, N and B atoms were refined anisotropically. Intensities for **3a** decayed ca. 5% during data collection and the data were scaled on the standard intensity ratios. All non-hydrogen atoms were refined anisotropically. The *i*Pr groups on N(3) are disordered and a model with two orientations (occupancies 62% and 38%) was employed. The H-atom on P(1) was located and its position was allowed to vary in the final refinement. Details on the crystal structure determination are deposited at the Cambridge Crystallographic Data Centre, 12 Union Road, Cambridge CB21EZ, England, and may be ordered by quoting the depository number CCDC-100383.

[1] A. Lang, H. Nöth, M. Thormann-Albach, *Chem. Ber.*, **1997**, *130*, 363−369.
[2] R. T. Paine, H. Nöth, *Chem. Rev.* **1995**, *95*, 343−379.
[3] D. Dou, G. L. Wood, E. N. Duesler, R. T. Paine, H. Nöth, *Inorg. Chem.* **1992**, *31*, 3756−3762.
[4] D. Dou, B. Kaufmann, E. N. Duesler, T. Chen, R. T. Paine, H. Nöth, *Inorg. Chem.* **1993**, *32*, 3056−3067.
[5] T. Chen, E. N. Duesler, R. T. Paine, H. Nöth, *Inorg. Chem.*, **1997**, *36*, 802−808.
[6] T. Chen, E. N. Duesler, R. T. Paine, H. Nöth, *Inorg. Chem.*, **1997**, *36*, 1070−1075.
[7] T. Chen, E. N. Duesler, R. T. Paine, H. Nöth, *Inorg. Chem.*, **1997**, *36*, 1534−1535.
[8] D. Dou, G. Linti, T. Chen, E. N. Duesler, R. T. Paine, H. Nöth, *Inorg. Chem.*, **1996**, *35*, 3626.
[9] W. Hönle, H. G. von Schnering, *Z. Anorg. Allg. Chem.*, **1978**, *442*, 91−94.
[10] K. F. Tebbe, T. Heinlein, *Z. Anorg. Allg. Chem.*, **1984**, *515*, 7−18.
[11] Sheldrick, G. M. *Nicolet SHELXTL Operations Manual*; Nicolet XRD Corp.: Cupertino, CA, 1981. SHELXTL uses absorption, anomalous dispersion, and scattering data compiled in *International Tables for X-Ray Crystallography*; Kynoch: Birmingham, England, **1974**; Vol. IV, pp. 55−60, 99−101, 149−150. Anomalous dispersion terms were included for all atoms with atomic numbers larger than 2.

[97001]